Fabrication and characterization of fibers with built-in liquid crystal channels and electrodes for transverse incident-light modulation

AIP | Applied Physics Letters

Fabrication and characterization of fibers with built-in liquid crystal channels and electrodes for transverse incident-light modulation

Alexander M. Stolyarov, Lei Wei, Fabien Sorin, Guillaume Lestoquoy, John D. Joannopoulos et al.

Citation: Appl. Phys. Lett. **101**, 011108 (2012); doi: 10.1063/1.4733319
View online: http://dx.doi.org/10.1063/1.4733319
View Table of Contents: http://apl.aip.org/resource/1/APPLAB/v101/i1
Published by the American Institute of Physics.

Fabrication and characterization of fibers with built-in liquid crystal channels and electrodes for transverse incident-light modulation

Alexander M. Stolyarov,[1,2,3] Lei Wei,[1,2] Fabien Sorin,[1,2,a)] Guillaume Lestoquoy,[1,2,4] John D. Joannopoulos,[1,2,5] and Yoel Fink[1,2,6,b)]
[1]*Research Laboratory of Electronics, Massachusetts Institute of Technology, 77 Massachusetts Avenue, Cambridge, Massachusetts 02139, USA*
[2]*Institute for Soldier Nanotechnologies, Massachusetts Institute of Technology, 77 Massachusetts Avenue, Cambridge, Massachusetts 02139, USA*
[3]*School of Engineering and Applied Sciences, Harvard University, 29 Oxford Street, Cambridge, Massachusetts 02138, USA*
[4]*Department of Electrical Engineering and Computer Science, Massachusetts Institute of Technology, 77 Massachusetts Avenue, Cambridge, Massachusetts 02139, USA*
[5]*Department of Physics, Massachusetts Institute of Technology, 77 Massachusetts Avenue, Cambridge, Massachusetts 02139, USA*
[6]*Department of Materials Science and Engineering, Massachusetts Institute of Technology, 77 Massachusetts Avenue, Cambridge, Massachusetts 02139, USA*

(Received 27 April 2012; accepted 16 June 2012; published online 5 July 2012)

We report on an all-in-fiber liquid crystal (LC) structure designed for the modulation of light incident transverse to the fiber axis. A hollow cavity flanked by viscous conductors is introduced into a polymer matrix, and the structure is thermally drawn into meters of fiber containing the geometrically scaled microfluidic channel and electrodes. The channel is filled with LCs, whose director orientation is modulated by an electric field generated between the built-in electrodes. Light transmission through the LC-channel at a particular location can be tuned by the *driving frequency of the applied field*, which directly controls the potential profile along the fiber. © *2012 American Institute of Physics*. [http://dx.doi.org/10.1063/1.4733319]

Photonic structures employing liquid crystals (LCs) are the subject of ongoing investigations. In addition to their ubiquitous presence in display technologies,[1] LCs are used to tailor laser emission,[2–5] in spatial light modulators,[6,7] as tunable wavelength filters,[8] and in a host of other applications.[9–13] In recent years, LC-infiltrated fiber structures have been explored for modulating *axially* propagating light through the application of externally generated fields.[14–18] Here, we report on the fabrication and characterization of a polymer fiber LC device for modulating *transversely* incident light. This regime of operation is particularly interesting for large-area flexible display applications, such as in fabrics. The fiber contains an axially uniform, rectangular LC-filled microchannel flanked on two opposing sides by built-in conductive polymeric electrodes. We investigate the effect of the applied voltage driving frequency on the transversely transmitted intensity as a function of fiber length. In accordance with our model, the high resistivity of the electrodes imposes an axial electric potential drop over a length controlled by the driving frequency. Therefore, by contacting the electrodes at multiple locations along their length, individual pixels along axially symmetric fibers could be addressed.

The fabrication of this fiber is realized by constructing a macroscopic version of the desired structure and subsequently scaling it down to the microscopic dimensions by thermal drawing. The fabrication process flow is depicted in Figs. 1(a)–1(c). Initially, 75 μm thick polycarbonate (PC, Lexan 104) is rolled onto a mandrel to a desired outer diameter and consolidated under vacuum at ~190 °C. Subsequently, a group of three parallel pockets are milled into the

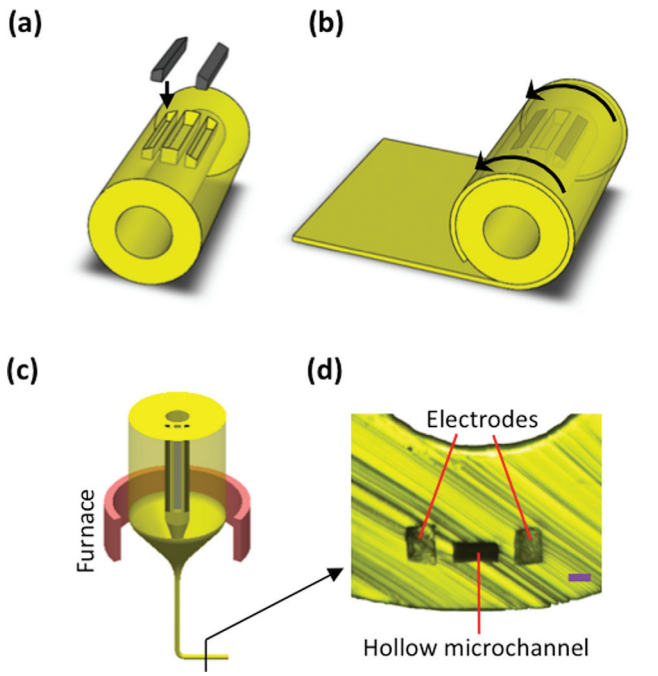

FIG. 1. Fiber fabrication. (a)-(c) Fabrication process flow and (d) Optical micrograph of the fiber structure containing a hollow microchannel flanked by conducting electrodes. Scale bar in (d) is 20 μm.

[a)]Present address: Laboratoire surface du verre et interfaces, Unité Mixte CNRS/Saint-Gobain UMR 125, 39 quai Lucien Lefranc, 93303 Aubervilliers, France.
[b)]Electronic mail: yoel@mit.edu.

structure at prescribed locations and dimensions. The outer two pockets are filled by geometrically matched strips of conductive carbon-loaded polyethylene (CPE), which are prepared through thermal pressing of individual 100 μm thick CPE films, and the central pocket is left empty. To confine the hollow pocket and neighboring conductors, the structure is clad with additional 75 μm thick PC films and reconsolidated. With the mandrel removed, the preform is thermally drawn at ~250 °C into hundreds of meters of flexible fiber containing a hollow microchannel flanked by conducting electrodes. The optical micrograph in Fig. 1(d) depicts the cross section of the fiber structure.

Post-draw, LCs (Merck MLC-2058, $n_e = 1.71$, $n_o = 1.51$ at 589 nm) are infiltrated into the microchannel through capillary action by dipping the fiber tip into a droplet of the LC mixture at room temperature. Although no alignment layer is applied to the microchannel walls prior to LC infiltration, the LC director orients itself along the fiber axis for several centimeters, as has also been observed in the microchannels of photonic crystal fibers.[18] (Note that since the index of refractive of polycarbonate ($n_{pc} = 1.58$) is lower than the extraordinary index of the LC, the LC channel could also function as a waveguide under an appropriate voltage bias and input polarization conditions, which we plan to investigate in future work.)

In this Letter, we explore the properties of the in-fiber LC channel as a variable attenuator for light transmitting perpendicular to its axis. The fiber is characterized in a microscope equipped with a bottom illuminator, polarizer and analyzer pair, and a top mounted CCD camera. The spatial arrangement of the setup is shown schematically in Fig. 2(a). Randomly polarized white light first passes through a polarizer with the transmission axis aligned perpendicular to the fiber axis. With the absence of an applied voltage, the linearly polarized light only interacts with the ordinary index of the LC, hence no change in polarization state occurs when the light passes through the fiber. Since the analyzer is fixed with its transmission axis aligned parallel to the fiber axis, no light is transmitted. Upon applying a voltage above a threshold voltage, the LC director rotates in the direction of the applied field, causing the incoming wave to experience both the ordinary and extraordinary indices of the LC molecules. This interaction leads to a change in the initial linear polarization state of the light passing through the microchannel, which translates into partial transmission through the analyzer.[19] An image captured on the CCD camera with the voltage off and on (100 V_{rms} at 100 Hz) is depicted in Fig. 2(b) for a 5-cm long fiber. Note that for this fiber length and driving frequency, the electrodes are equipotential along their entire length. Figure 2(c) displays the dependence of the transmission intensity on driving voltage, demonstrating continuous tunability of the transversely transmitted intensity. No change in transmission is observed below a threshold voltage of ~25 V. Above 25 V, the transmission increases with increasing voltage up to the maximum applied voltage of 140 V. Note that if the applied voltage would continue to grow, we expect the transmission to reach a maximum (when the LC director is oriented at 45° relative to the fiber axis) and then begin to decrease back to zero as the LC director approaches 90°. Although the limitations of our

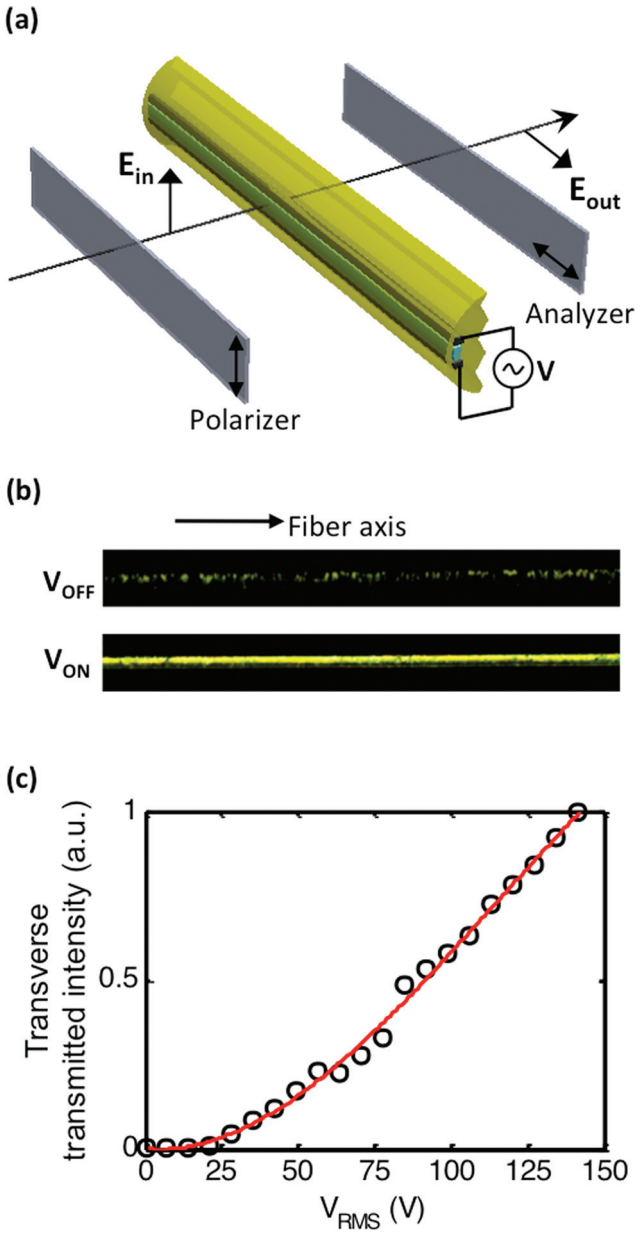

FIG. 2. Characterization of the in-fiber LC channel. (a) Schematic of the experimental setup used to measure light transmitting though the LC-channel normal to the fiber axis. The voltage is applied directly to the in-fiber electrodes (black) which flank the LC-channel (blue) (b) Images of the fiber with voltage OFF (0 V) and ON (100 V). The randomly distributed white specks seen in the OFF state arise from imperfections in the LC alignment near the microchannel wall. (c) A characteristic transmission vs. applied voltage spectrum obtained at a driving frequency of 100 Hz. The red curve is an empirical fit to the data using a 6th order polynomial. (Note that the sole purpose of this polynomial function is to relate the experimentally measured transmission dependence on the applied voltage, which we use in Fig. 3(d).)

voltage source precluded measuring this full transmission range, we have observed a saturation in transmission intensity when characterizing fibers in which the electrodes are separated by a slightly smaller distance. (see supplemental Fig. 1).[25]

An interesting feature of this LC channel emerges when considering extended fiber lengths. The CPE electrodes and the PC-enclosed LC channel which they flank form a distributed RC circuit in a transmission line fashion, in which each unit length of fiber Δz has a series resistance from the CPE

electrodes (R_{CPE}) and a parallel capacitance from the PC and LC (C_{eq}). These can be estimated from the structure as illustrated in Fig. 3(a) and are expressed as

$$C_{eq} = \varepsilon_{PC}\left[\frac{w_E}{2h_{PC}+h_{LC}} + \frac{h_{LC}(1-\varepsilon_{PC}/\varepsilon_{LC})w_{LC}}{(2h_{PC}+h_{LC})\left(2h_{PC}+h_{LC}(\varepsilon_{PC}/\varepsilon_{LC})\right)}\right]\Delta z \ , \quad (1)$$

$$R_{CPE} = [\rho(h_E w_E)^{-1}]\Delta z \quad . \quad (2)$$

By applying Kirchoff's laws to the distributed circuit along the fiber length, the electric potential along the electrodes a distance z away from the point where they are contacted can be expressed as[20]

$$V(z) = \frac{V_0 \cosh\left(\frac{L-z}{\delta}\right)}{\cosh\left(\frac{L}{\delta}\right)} \quad (3)$$

with

$$\delta = \sqrt{\frac{(\Delta z)^2}{i4\pi f R_{CPE} C_{eq}}} \quad , \quad (4)$$

where V_0 and f are, respectively, the amplitude and driving frequency (in Hz) of the applied voltage, while L is the length from the point of electrode contact to the end of the fiber. Since the transfer length δ depends on frequency, it follows that $V(z)$ and hence the light transmission at a particular location away from the point of electrical contact is also frequency dependent.

Figure 3(b) depicts a surface plot of the calculated voltage dependence on driving frequency and position along the axis of a 40-cm long fiber that is contacted at the 0-cm end. Evident in this plot is the voltage decay towards longer distances and higher frequencies, a consequence primarily of the high CPE resistivity ($\rho_{CPE} \approx 1.1\ \Omega$m). While, on the one hand, this voltage drop limits the driving frequency on long fibers that are electrically contacted at one location, it presents an opportunity on the other. Since the CPE electrodes can be electrically contacted at multiple locations along their length, the rapid voltage decay at a typical LC driving frequency of 1 kHz actually facilitates independent and simultaneous control over multiple sections of the same LC channel, a function that is particularly useful for display applications. Note that if an uniform voltage is desired along the entire fiber length (which would be useful, for example, in the aforementioned waveguide implementation of the LC channel), metallic electrodes (such as eutectic alloy $Bi_{58}Sn_{42}$ or indium) can be drawn in place of or in direct contact with the conductive polymer inside PC-clad fibers.[21,22] Having a resistivity about 8 orders of magnitude lower than CPE, the metallic electrodes will maintain the same electric potential

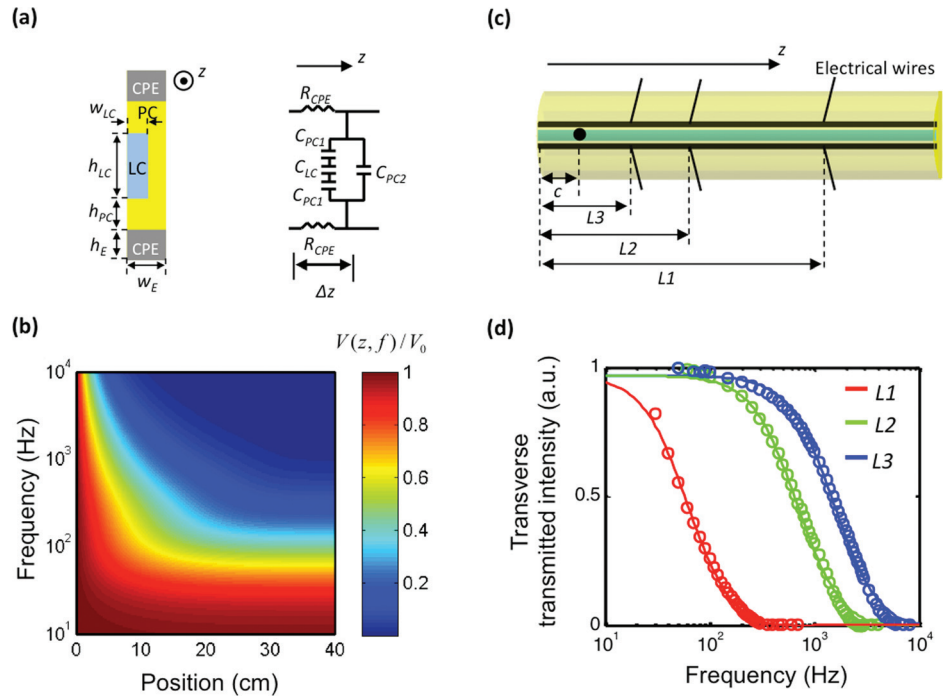

FIG. 3. Characterization of the LC channel frequency response. (a) (left) Cross section schematic of the LC channel and neighboring electrodes (see Fig. 1(d)). (right) Equivalent circuit for an unit fiber segment length Δz used to analyze the frequency response. The structural and materials parameters used in this study are the following: $W_E = 30\ \mu$m, $W_{LC} = 17\ \mu$m, $h_{LC} = 35\ \mu$m, $h_{PC} = 14\ \mu$m, and $h_E = 23\ \mu$m. The resistivity ρ of CPE is experimentally determined to be ~1.1 Ωm. The dielectric constants of the LC (Ref. 24) and PC are taken as $\varepsilon_{LC} = 13$ and $\varepsilon_{PC} = 3$. (b) Surface plot of the calculated electric potential as a function of frequency and position along the fiber axis for a 40-cm long fiber that is contacted at the 0-cm side. (c) Schematic of the experiment used to test the model derived from the equivalent circuit in (a). The distance between the point of electrical contact to the electrodes (denoted by a pair of slightly angled black lines) and the end of the fiber is 35 cm, 10.5 cm, and 7 cm, corresponding to *L1*, *L2*, and *L3*, respectively. The black dot (a distance c (1 cm) from the fiber end) corresponds to the location where the light transmission is measured in (d). (d) Transmission intensity measurements for driving the electrodes at positions *L1*, *L2*, and *L3* as a function of frequency. Open circles and solid lines correspond to the measured and calculated values, respectively. To calculate the transmission as a function of frequency, Eq. (3) is first used to determine the voltage as a function of frequency at point c. The voltage is then converted into the corresponding transmission intensity by using the polynomial fit from the measurement depicted in Fig. 2(c).

along the entire 40-cm fiber length at frequencies of 1 kHz and lower (see supplemental Fig. 2).

To demonstrate the driving frequency as a control knob for tuning the transmission intensity as a function of position, we contact an electrode pair of a 40-cm long fiber at three different locations as depicted in Fig. 3(c).[23] For each of the three experiments ($L = L1, L2$, and $L3$), 125 V are applied to the electrodes at point L, and the transmission intensity is recorded at point c as the frequency is varied in the range of 30–10^4 Hz. Figure 3(d) displays the measured frequency-dependent transmission (open circles); the calculated transmission curves (solid lines) based on our model agree well with the data. Note that at a driving frequency of 1 kHz, the applied voltage at *L1* has no influence over the transmission at point c, in contrast to applying the voltage at *L3* and *L2*. As noted previously, this localized control over the LC response presents an intriguing opportunity for driving multiple sections of the same LC channel.

In summary, we have reported on an in-fiber LC structure designed for modulation of light incident transversely to its axis. Viscous conductive electrodes used to address the LC channel are built directly into the fiber cladding. We demonstrated the transverse-transmission intensity at a particular location along the LC channel could be controlled by the driving frequency of the applied voltage, which allows for localized light attenuation control along axially symmetric fibers.

A.M.S is thankful for the support of the NSF Graduate Research Fellowship. L.W. is grateful for the support from Technical University of Denmark. This work was supported in part by the Materials Research Science and Engineering Program of the US National Science Foundation under Award No. DMR-0819762 and also in part by the US Army Research Office through the Institute for Soldier Nanotechnologies under Contract No. W911NF-07-D-0004.

[1]H. Kawamoto, Proc. IEEE **90**, 460 (2002).
[2]R. Ozaki, T. Matsui, M. Ozaki, and K. Yoshino, Appl. Phys. Lett. **82**, 3593 (2003).
[3]B. Maune, M. Lončar, J. Witzens, M. Hochberg, T. B. Jones, D. Psaltis, A. Scherer, and Y. Qiu, Appl. Phys. Lett. **85**, 360 (2004).
[4]G. Strangi, V. Barna, R. Caputo, A. De Luca, C. Versace, N. Scaramuzza, C. Umeton, R. Bartolino, and G. N. Price, Phys. Rev. Lett. **94**, 063903 (2005).
[5]A. M. Stolyarov, L. Wei, O. Shapira, F. Sorin, S. L. Chua, J. D. Joannopoulos, and Y. Fink, Nature Photon. **6**, 229 (2012).
[6]G. D. Love, Appl. Opt. **36**, 1517 (1997).
[7]N. Konforti, E. Marom, and S.-T. Wu, Opt. Lett. **13**, 251 (1988).
[8]J. S. Patel, M. A. Saifi, D. W. Berreman, C. Lin, N. Andreakis, and S. D. Lee, Appl. Phys. Lett. **57**, 1718 (1990).
[9]H. Meyer, D. Riekmann, K. P. Schmidt, U. J. Schmidt, M. Rahlff, E. Schrbder, and W. Thust, Appl. Opt. **11**, 1732 (1972).
[10]S. Sato, Jpn. J. Appl. Phys., Part 1 **18**, 1679 (1979).
[11]A. Fratalocchi and G. Assanto, Opt. Lett. **29**, 1530 (2004).
[12]M. Humar, M. Ravnik, S. Pajk, and I. Muševič, Nat. Photonics **3**, 595 (2009).
[13]M. Oh-e and K. Kondo, Appl. Phys. Lett.**67**, 3895 (1995).
[14]T. Larsen, A. Bjarklev, D. Hermann, and J. Broeng, Opt. Express **11**, 2589 (2003).
[15]T. Alkeskjold, J. Lægsgaard, A. Bjarklev, D. Hermann, A. Anawati, J. Broeng, J. Li, and S. T. Wu, Opt. Express **12**, 5857 (2004).
[16]F. Du, Y. Q. Lu, and S. T. Wu, Appl. Phys. Lett. **85**, 2181 (2004).
[17]M. W. Haakestad, T. T. Alkeskjold, M. D. Nielsen, L. Scolari, J. Riishede, H. E. Engan, and A. Bjarklev, IEEE Photon. Technol. Lett. **17**, 819 (2005).
[18]T. T. Alkeskjold, L. Scolari, D. Noordegraaf, J. Lægsgaard, J. Weirich, L. Wei, G. Tartarini, P. Bassi, S. Gauza, S.-T. Wu, and A. Bjarklev, Opt. Quantum Electron. **39**, 1009 (2007).
[19]P. Yeh and C. Gu, *Optics of Liquid Crystal Displays*, 2nd ed. (Wiley, Hoboken, 2010).
[20]F. Sorin, G. Lestoquoy, S. Danto, J. D. Joannopoulos, and Y. Fink, Opt. Express **18**, 24264 (2010).
[21]N. Chocat, G. Lestoquoy, Z. Wang, D. N. Rodgers, J. D. Joannopoulos, and Y. Fink, "Piezoelectric fibers for conformal acoustics," Adv. Mater. (to be published).
[22]S. Egusa, Z. Wang, N. Chocat, Z. M. Ruff, A. M. Stolyarov, D. Shemuly, F. Sorin, P. T. Rakich, J. D. Joannopoulos, and Y. Fink, Nature Mater. **9**, 643 (2010).
[23]Fixing the transmission location and varying its spacing from the point of electrode contact is equivalent to fixing the point of electrode contact and varying the position where transmission is measured. We find that the uniformity of the LC director alignment decreases with increasing distance away from the fiber facet (i.e., where the LC is introduced into the microchannel), therefore we perform the former experiment and choose a transmission location close to the fiber facet (1 cm away). Improved LC infiltration methods for realizing longer homogeneously aligned in-fiber LC cells are currently under investigation.
[24]Due to the dielectric anisotropy of the LC ($\varepsilon_{\text{parallel}} = 21.2$ and $\varepsilon_{\text{perpendicular}} = 4.7$), the value of ε in the direction orthogonal to the electrodes changes as a function of the LC director orientation. However, it is the ε_{PC} that plays the dominant role in the equivalent capacitance of the structure; hence, variations of ε_{LC} will only slightly affect the frequency response. For the calculations shown in Fig. 3, the average value for ε_{LC} is used, i.e., $\varepsilon_{LC} = 13$.
[25]See supplementary material at http://dx.doi.org/10.1063/1.4733319 for additional data.